



OPEN ACCESS

Original research

# From clinical variables to multiomics analysis: a margin morphology-based gross classification system for hepatocellular carcinoma stratification

Zhongqi Fan,<sup>1</sup> Meishan Jin,<sup>2</sup> Lei Zhang,<sup>3</sup> Nanya Wang,<sup>4</sup> Mingyue Li,<sup>1</sup> Chuanlei Wang,<sup>1</sup> Feng Wei,<sup>1</sup> Ping Zhang,<sup>1</sup> Xiaohong Du,<sup>1</sup> Xiaodong Sun,<sup>1</sup> Wei Qiu,<sup>1</sup> Meng Wang,<sup>1</sup> Hongbin Wang,<sup>3</sup> Xiaojun Shi,<sup>1</sup> Junfeng Ye,<sup>1</sup> Chao Jiang,<sup>1</sup> Jianpeng Zhou,<sup>1</sup> Wengang Chai,<sup>1</sup> Jun Qi,<sup>1</sup> Ting Li,<sup>1</sup> Ruoyan Zhang,<sup>1</sup> Xingkai Liu,<sup>1</sup> Bo Huang,<sup>1</sup> Kaiyuan Chai,<sup>1</sup> Yannan Cao,<sup>1</sup> Wentao Mu,<sup>1</sup> Yu Huang,<sup>1</sup> Tian Yang <sup>5</sup>, Huimao Zhang,<sup>3</sup> Limei Qu,<sup>2</sup> Yahui Liu,<sup>1</sup> Guangyi Wang,<sup>1</sup> Guoyue Lv <sup>1</sup>

► Additional supplemental material is published online only. To view, please visit the journal online (<http://dx.doi.org/10.1136/gutjnl-2023-330461>).

<sup>1</sup>Department of Hepatobiliary and Pancreatic Surgery, General Surgery Center, The First Hospital of Jilin University, Changchun, Jilin, China

<sup>2</sup>Department of Pathology, The First Hospital of Jilin University, Changchun, Jilin, China

<sup>3</sup>Department of Radiology, The First Hospital of Jilin University, Changchun, China

<sup>4</sup>Phase I Clinical Trials Unit, The First Hospital of Jilin University, Changchun, Jilin, China

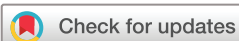
<sup>5</sup>Department of Hepatobiliary Surgery, Eastern Hepatobiliary Surgery Hospital, Shanghai, China

## Correspondence to

Guoyue Lv, Department of Hepatobiliary and Pancreatic Surgery, General Surgery Center, The First Hospital of Jilin University, Changchun 130021, China; [lvgy@jlu.edu.cn](mailto:lvgy@jlu.edu.cn)

ZF and MJ contributed equally.

Received 9 June 2023  
Accepted 20 July 2023  
Published Online First  
7 August 2023



© Author(s) (or their employer(s)) 2023. Re-use permitted under CC BY-NC. No commercial re-use. See rights and permissions. Published by BMJ.

**To cite:** Fan Z, Jin M, Zhang L, *et al.* *Gut* 2023;**72**:2149–2163.

## ABSTRACT

**Objective** Selecting interventions for patients with solitary hepatocellular carcinoma (HCC) remains a challenge. Despite gross classification being proposed as a potential prognostic predictor, its widespread use has been restricted due to inadequate studies with sufficient patient numbers and the lack of established mechanisms. We sought to investigate the prognostic impacts on patients with HCC of different gross subtypes and assess their corresponding molecular landscapes.

**Design** A prospective cohort of 400 patients who underwent hepatic resection for solitary HCC was reviewed and analysed and gross classification was assessed. Multiomics analyses were performed on tumours and non-tumour tissues from 49 patients to investigate the mechanisms underlying gross classification. Inverse probability of treatment weight (IPTW) was used to control for confounding factors.

**Results** Overall 3-year survival rates varied significantly among the four gross subtypes (type I: 91%, type II: 80%, type III: 74.6%, type IV: 38.8%). Type IV was found to be independently associated with poor prognosis in both the entire cohort and the IPTW cohort. The four gross subtypes exhibited three distinct transcriptional modules. Particularly, type IV tumours exhibited increased angiogenesis and immune score as well as decreased metabolic pathways, together with highest frequency of TP53 mutations. Patients with type IV HCC may benefit from adjuvant intra-arterial therapy other than the other three subtypes. Accordingly, a modified trichotomous margin morphological gross classification was established.

**Conclusion** Different gross types of HCC showed significantly different prognosis and molecular characteristics. Gross classification may aid in development of precise individualised diagnosis and treatment strategies for HCC.

## INTRODUCTION

Hepatocellular carcinoma (HCC) is the most common cancer of hepatobiliary system and remains as one of the leading causes of cancer-related death.

## WHAT IS ALREADY KNOWN ON THIS TOPIC

- ⇒ The accuracy of various staging systems for solitary hepatocellular carcinoma (HCC) in guiding treatment decisions and predicting prognosis remains limited.
- ⇒ Gross classification can predict the prognosis of patients undergoing hepatic resection for small solitary HCC, but it is not widely used in clinical practice.
- ⇒ A few stemness and fibrotic stroma marker genes are differently expressed in HCCs with each gross subtype.

## WHAT THIS STUDY ADDS

- ⇒ The gross classification is validated as an effective factor in predicting prognosis in patients with HCC using a relatively large prospective cohort and the inverse probability of treatment weight method to eliminate potential confounding effects.
- ⇒ Distinct molecular expression patterns, gene mutations and components of tumour microenvironment (TME) are discovered among the four gross subtypes.
- ⇒ Infiltrative type HCC exhibits the most similarities to intrahepatic cholangiocarcinoma in terms of gross appearance, prognosis and downregulated expression profiles.
- ⇒ Only infiltrative type HCC shows response to adjuvant transcatheter arterial chemoembolisation (TACE).
- ⇒ An easy-to-use modified gross classification system (MMC) for HCC based solely on margin morphology is proposed.

Although the prognosis of patients with HCC has improved significantly with rapidly evolving in various therapeutic strategies, recurrence remains as the main challenge in the management of HCC. Local therapies, including surgery, radiofrequency ablation (RFA) and transcatheter arterial chemoembolisation (TACE), considered as standard care

**HOW THIS STUDY MIGHT AFFECT RESEARCH, PRACTICE OR POLICY**

- ⇒ Gross classification of HCC is supported by both clinical and molecular rationales, making it a comprehensive and reliable method for stratifying patients. A priority assessment for infiltrative type in treatment decision-making is recommended.
- ⇒ Adjuvant TACE should be performed in infiltrative type HCC following hepatectomy.
- ⇒ The components of immune TME in each gross subtype, which can be evaluated by imaging, may provide evidence to choose the optimal immunotherapy-based strategy for advance HCC.
- ⇒ MMC can improving the clinical applicability of gross classification for HCC.
- ⇒ More attention should be paid on macroscopic features of all tumours, instead of focusing solely on microscopic features.

for early-stage or intermediate HCC are recommended by many guidelines,<sup>1-3</sup> but clinical studies comparing these interventions have not reached consistent conclusions.<sup>4</sup> The dilemma of choosing interventions persists for HCC, especially for the cases with single nodule. There is still a lack of a non-invasive and simple indicator of prognosis together with aiding in clinical decision-making in HCC. On the other hand, atezolizumab plus bevacizumab was confirmed to provide survival benefits for patients with advanced HCC.<sup>5</sup> To date, no promising biomarkers of response to the first-line therapy have been identified.<sup>6,7</sup>

There is an old adage in pathological diagnosis that goes ‘macroscopy accounts for 70%, microscopy accounts for 30%’. Typically, the gross pathology of HCC is often simplistically equated with the size, number or texture of the lesions. In 1987, Moriyama’s group classified HCC into five gross subtypes based primarily on tumour shape: single nodular type (type I), single nodular type with extranodular growth (type II), contiguous multinodular type (type III), poor demonstrated type (also named as infiltrative type, type IV) and early HCC type.<sup>8</sup> Several limited retrospective studies have suggested a correlation between tumour shape and prognosis in patients with HCC,<sup>8-11</sup> even imaging features reflecting HCC gross appearance have been proposed to be predictive of outcomes after RFA, TACE,

even treated with lenvatinib.<sup>12,13</sup> Despite the utility of the classification system for HCC, its clinical implementation has been limited due to diagnostic challenges associated with certain subtypes and a scarcity of cases representing each subtype that would facilitate robust clinical investigation.<sup>14,15</sup> Describing the molecular landscape of HCC subtypes can help explain the rationale behind this classification and expedite its optimisation.

Primarily using a prospective cohort of patients undergoing hepatectomy for different gross subtypes HCC, we sought to investigate the role of tumour morphology in oncological survival. Integrative multiomics analyses were employed to portray the molecular landscapes among distinct HCC gross subtypes and optimise the classification system, culminating in the development of a margin morphology classification (MMC) system. The current study can establish a strong foundation for informed precise and effective personalised therapies of patients with HCC, particularly those with a single nodule when imaging can accurately depict the margin morphology of the tumour.

**MATERIALS AND METHODS**

**Gross classification**

The gross classification of resected HCC was separately assessed by one surgeon and one pathologist mainly according to the definition raised by Liver Cancer Study Group of Japan.<sup>8,16</sup> Details are as follows: type I: single nodule with distinct margin, usually round with complete tumour envelope; type II: single nodule with extranodular growth, no more than three extranodular points; type III: a unifocal lesion composed of confluent multiple nodules, distinct boundaries among the nodules; type IV: infiltrative nodule, with poor demarcated boundary and especially multiple extranodular points. The gross morphology of multi-layered tumour specimens before and after formalin fixation were both included to be evaluated, and we also referred to the imaging features at the largest tumour dimension to ensure the credibility of the gross classification (figure 1A,B).

**Study population and tumour samples**

A prospective cohort of patients who underwent hepatectomy for HCC from 2017 to 2021 at First Hospital of Jilin University was constructed, and was retrospectively analysed. The inclusion criteria were patients: (1) had HCC which was confirmed by pathological examination of resected specimens; (2) had

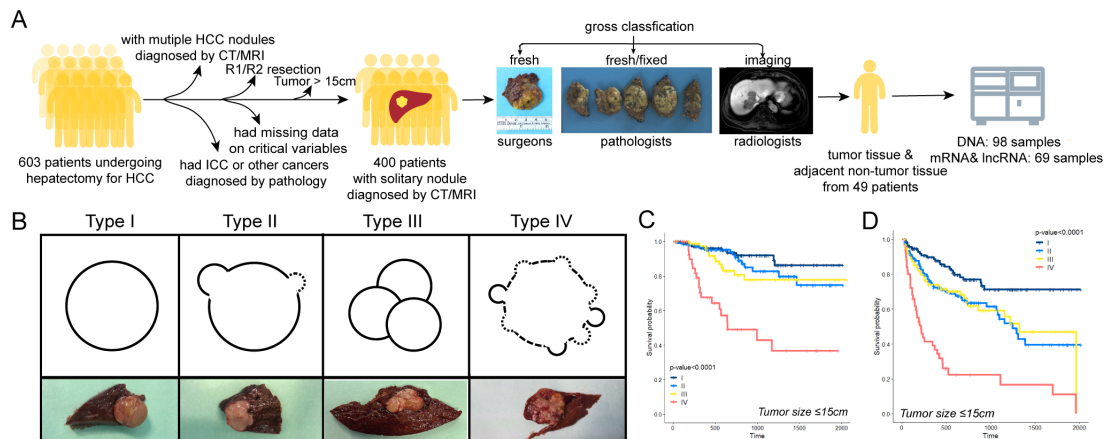


**Figure 1** The prognosis of patients with HCC varies depending on their gross subtype. (A) Flow chart of the study. (B) Different gross types of HCC and their corresponding fresh surgical resected samples. (C) Kaplan-Meier curves for OS based on the gross type in the current cohort (log-rank test). (D) Kaplan-Meier curves for RFS on the basis of the gross type in the current cohort (log-rank test). HCC, hepatocellular carcinoma; ICC, intrahepatic cholangiocarcinoma; OS, overall survival; RFS, recurrence-free survival.

single HCC nodule detected by CT/MRI imaging and (3) no extrahepatic spread. The exclusion criteria were patients who: (1) had HCC nodule >15 cm; (2) with multiple HCC nodules diagnosed by imaging; (3) with ruptured and recurrent HCC; (4) with palliative surgical resection (R1 or R2 resection); (5) with intrahepatic cholangiocarcinoma (ICC) or other malignant tumours diagnosed pathologically; (6) had perioperative death ( $\leq 30$  days); (7) had inconsistency in determining the gross classification of HCC between surgeons and pathologists and (8) had missing data on essential variables. Another prospective cohort of patients with advanced HCC who received immunotherapy combined with antiangiogenesis targeted therapy ( $\geq 2$  cycles) was also enrolled. Residual surgical excision specimens for pathological diagnosis were collected and stored in  $-80^{\circ}\text{C}$  freezer. Samples were consecutively collected from 12 to 13 patients for each gross subtype, resulting in a total of 49 patients with solitary HCCs measuring  $\leq 5$  cm in diameter. Total RNA and DNA were isolated from each sample for subsequent whole-genome sequencing and expression analysis. Whole-genome sequencing analysis was conducted on 49 paired tissues from the 49 patients. Additionally, expression analysis was performed on a subset of 69 samples including 39 tumour tissues and 30 were non-tumour tissues from 39 patients (figure 1A). Notably, the collected samples did not include any capsular tissues. The non-tumour tissues used for sequencing were identified as free from contamination with tumour tissues by histology.

A detailed description of other methods used in current study can be found in online supplemental methods.

## RESULTS

### Strong differences in prognosis across the four gross subtypes of HCC

The patient flow chart is presented in figure 1A. Among the 400 patients undergoing hepatic resection for HCC with single nodule, 280 (70.0%) were hepatitis B virus (HBV)-related individuals. With a median follow-up of 25.5 months, 67 of 396 patients (16.9%) died, and 147 (37.4%) developed recurrence of HCC. A total of 52 (13.0%) individuals had type IV nodules, while 118 (29.5%), 129 (32.3%) and 101 (25.3%) had HCCs belonging to type I, type II and type III nodules, respectively. The comparisons of clinicopathological characteristics and operative variables among patients with different gross types of HCC are noted in online supplemental table 1. In type IV group, the proportions of patients with microvascular invasion (88.4%), macrovascular invasion (48.1%) and satellite nodules (40.4%) and HBV infection (92.3%) were significantly higher than patients in other three groups (all  $p < 0.001$ ). Meanwhile, type IV tumours were found with larger tumour size, poorer differentiation and less complete tumour capsule than other three types HCC (all  $p < 0.001$ ). The proportions of patients with HCC with type IV at BCLC C stage (61.5%) were significantly higher than other subtypes (10.2%, 14.7% and 13.9% for types I, II, III respectively;  $p < 0.001$ ). HCC notably, the significant linear-by-linear association demonstrated that a progressive change in type IV compared with types I, II and III (all  $p < 0.001$ , online supplemental table 1). Other variables were comparable among different gross types (all  $p > 0.05$ ). The patients with type I HCCs had superior overall survival (OS) and recurrence-free survival (RFS) than patients with type II or III, with type IV demonstrating the worst prognosis (figure 1C,D;  $p < 0.0001$ ). Similar trends were also found in subgroup analyses enrolling patients with  $\leq 5$  cm HCC or with HBV-related HCC (online supplemental figure 1).

### Distinct transcriptomic profiles among the four gross subtypes of HCC

To gain a better understanding of the underlying mechanisms involved in gross classification and to clarify the rationale for molecular-level gross classification, mRNA, lncRNA and protein expression levels were detected using transcriptomics and proteomics methods in tumour ( $\leq 5$  cm) and non-tumour samples (figure 2, online supplemental figure 2–5). The results showed that HCCs with type III and types IV had more differentially expressed genes (DEGs) than those in type I or type II group (figure 2A,B). Hierarchical clustering revealed that type II and type III HCCs had similar expression patterns, while type I or type IV HCCs had less expressional overlaps with other types (figure 2C). Furthermore, simplified enrichment analysis of DEGs was performed to cluster functional enrichment results. Type II and type III HCCs were characterised by downregulated immune-related pathways, including leucocyte activation and cytokine production. Type IV HCCs exhibited markedly downregulated metabolic pathways and lipid transport, together with upregulated biogenesis and nucleocytoplasmic transport (figure 2D,E, online supplemental figure 6 and 7), which was also demonstrated at the protein level (online supplemental figure 5). The relative gene expression patterns across gross subtypes were calculated by GSVA, while ESTIMATE and xCell were used to evaluate the abundance of immune and stromal cells. The four gross subtypes had three main expression modules, whereas type II and type III HCCs shared similar expression characteristics (figure 2F–I and online supplemental figure 8). HCCs with type IV exhibited significantly higher stromal scores (figure 2J) and a higher median immune score than HCCs with other types (figure 2K). A high presence of  $\text{CD4}^{+}$  and  $\text{CD8}^{+}$  T effector memory cells was found in type I, and the increased abundance of fibroblasts in type IV was calculated (online supplemental figure 9).

### Type IV as an independent risk factor for HCC with special transcriptional characteristics

The worse prognosis remained in type IV HCC compared with other three gross subtypes after using stabilised inverse probability of treatment weight (IPTW) to balance the distribution of baseline characteristics due to possible selection bias among patients (figure 3A–D, online supplemental table 2). Subsequently, the univariate and multivariate Cox-regression analyses of risk factors for OS and RFS were performed for patients undergoing hepatic resection of HCC with type IV and other subtypes. Multivariate analyses demonstrated that type IV was independently associated with poorer OS after hepatectomy (HR 2.50, 95% CI 1.37 to 4.56,  $p = 0.003$ ), as well as poorer RFS (HR 1.65, 95% CI 1.05 to 2.60,  $p = 0.031$ ), respectively (figure 3E,F). Although some common pathways, such as spindle and condensed chromosome-related cellular components, were enriched across all subtypes, type IV HCC exhibited a higher number of gene counts and more invasion-related pathways, including focal adhesion and cell leading edge (figure 3G). Compared with non-tumour tissues, HCC with type IV was showed with enhanced angiogenesis, epithelial mesenchymal transition (EMT) and protein secretion using GSEA, which were shown with opposite expression patterns in other groups (figure 3H–L and online supplemental figure 10). Given that the gross appearance of HCCs with type IV is indistinguishable from ICC and both have shortened patient prognosis, we investigated whether they shared comparable expression

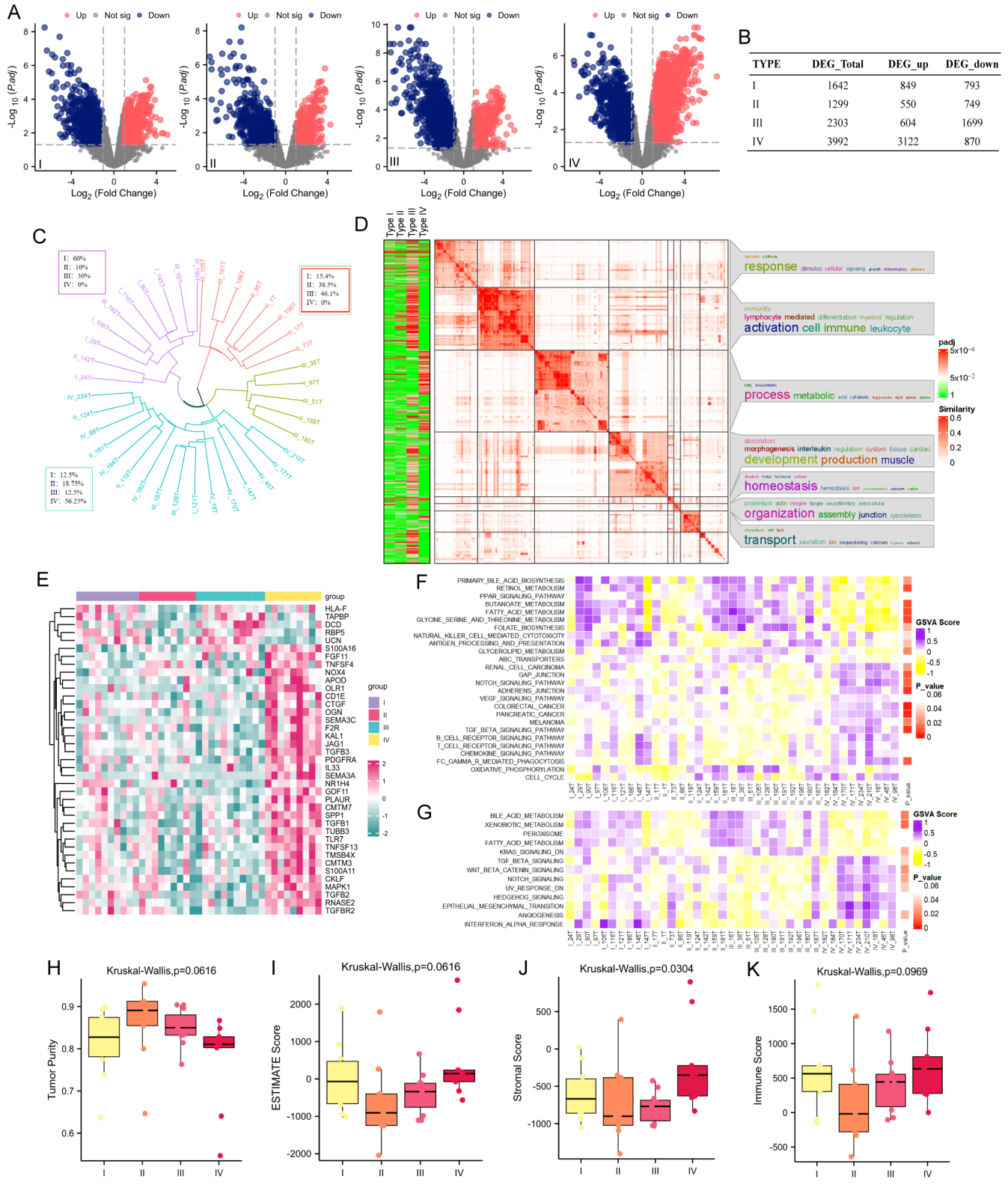


**Figure 2** Different HCC subtypes exhibit distinct mRNA expression profiles. (A) Volcano plot for DEGs between tumour tissues and non-tumour tissues in each gross subtype. Not sig, not significantly. (B) The numbers of DEGs among the four gross subtypes. (C) Polar dendrogram based on hierarchical clustering of the mRNA expression profiling. The proportions of different gross types in the three general clusters were shown. (D) Simplify enrichment analysis of downregulated DEGs between tumour tissues and non-tumour tissues in the four gross subtypes ( $p < 0.05$ ). (E) Heatmap for mRNA expression of immune related genes. (F, G) Heatmap depicting GSVA scores of KEGG gene sets and hallmark gene sets (Kruskal-Wallis test). (H–K) Box plots demonstrating differences in tumour purity, ESTIMATE score, stromal score and immune score calculated via ESTIMATE across the four gross subtypes (Kruskal-Wallis test). DEGs, differentially expressed genes; GSVA, gene set variation analysis; HCC, hepatocellular carcinoma.

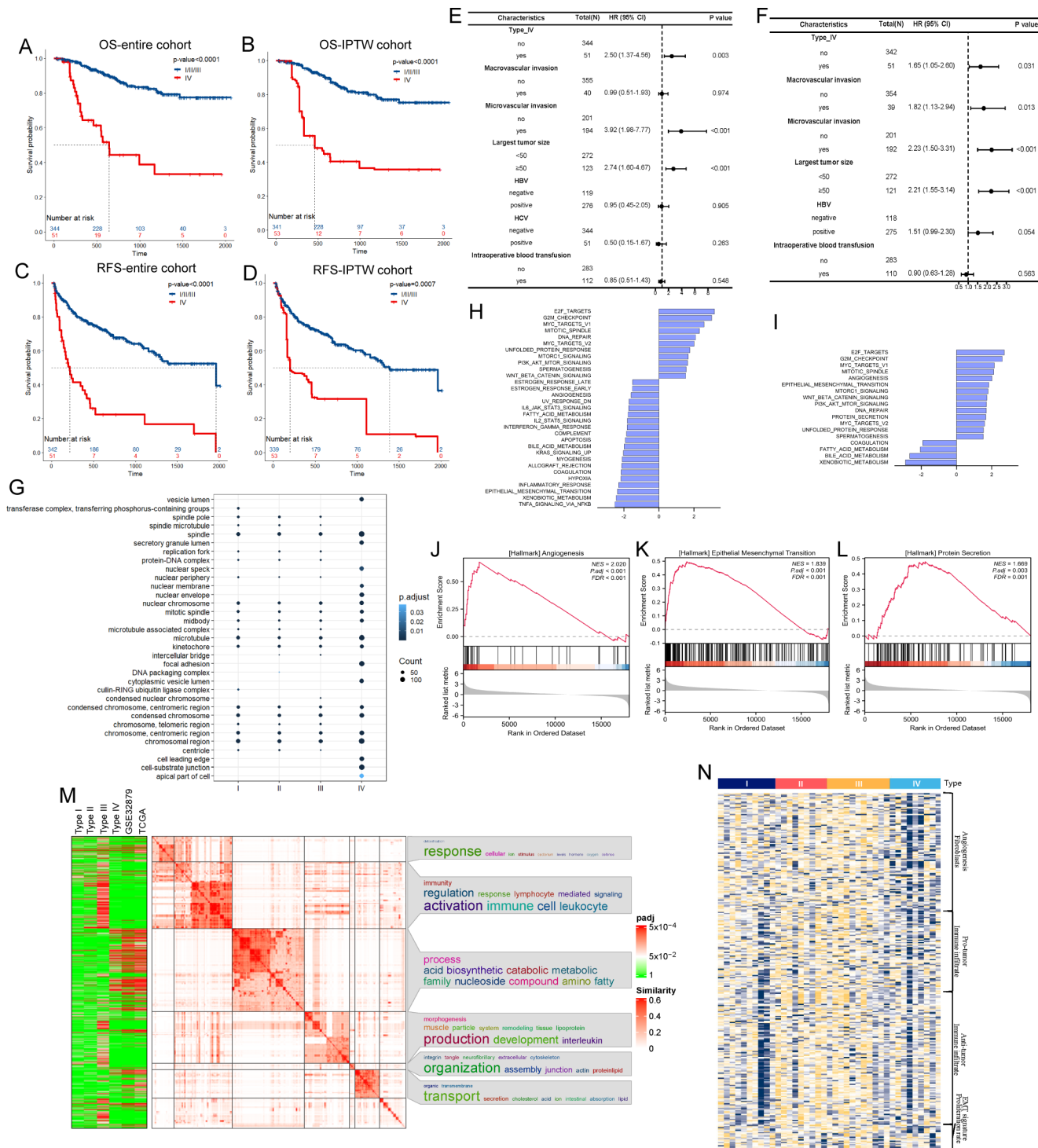


**Figure 3** Type IV as an independent prognostic risk factor for HCC with particular transcriptional characteristics. (A, B) Kaplan-Meier curves for OS for patients with type IV tumours versus type I/III/III tumours in indicated cohort (log-rank test). (C, D) Kaplan-Meier curves for RFS for patients in type IV group versus type I/III/III group in indicated cohort (log-rank test). (E, F) Forest map showing multivariate Cox-regression analysis of risk factors for OS and RFS. (G) Dot plot showing GO cellular component enrichment analysis of upregulated DEGs in each gross type. (H) GSEA based on mRNA expression of type I tumours versus corresponding non-tumours using hallmark gene sets (p < 0.05). (I) GSEA using hallmark gene sets based on mRNA expression of type IV tumours versus related non-tumours (p < 0.05). (J–L) GSEA plots of the indicated signature for type IV tumours versus type I/III/III tumours. (M) Simplify enrichment analysis based on downregulated DEGs between tumour tissues and non-tumour tissues among the four types in current HCC cohort as well as in published ICC cohorts (TCGA-CHOL and GSE32879). (N) Heatmap for mRNA expression of genes involved in indicated tumour microenvironment signatures raised by Bagaev A among the four gross subtypes.<sup>17</sup> DEGs, differentially expressed genes; FDR, false discovery rates; HBV, hepatitis B virus; HCC, hepatocellular carcinoma; ICC, intrahepatic cholangiocarcinoma; IPTW, inverse probability of treatment weight; NES, normalised enrichment score; OS, overall survival; RFS, recurrence-free survival.

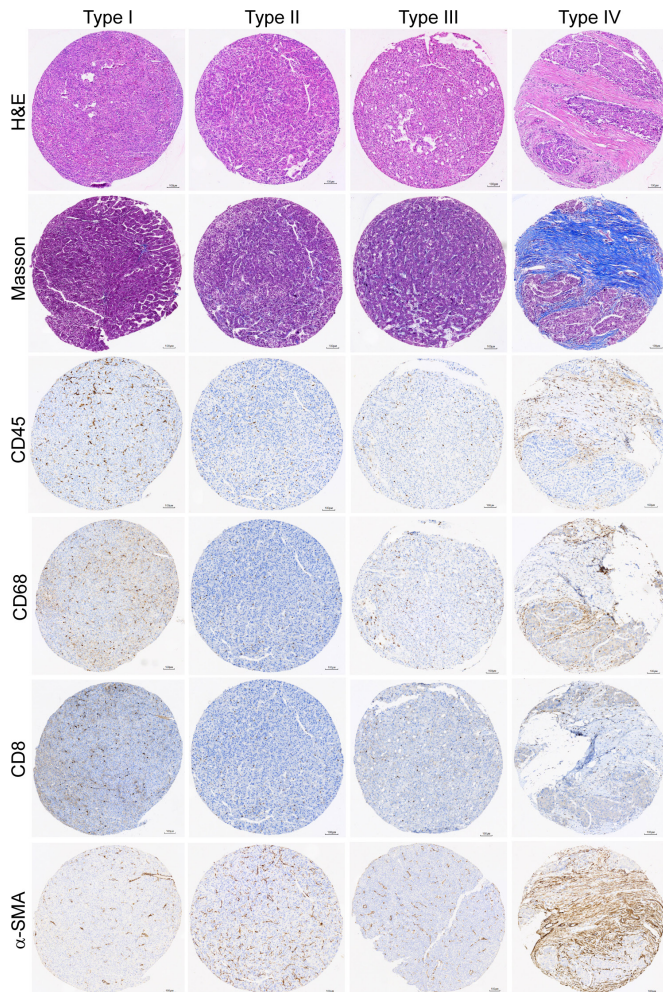


**Figure 4** Different gross subtype HCC is shown with distinct TME histologically. Representative H&E staining, Masson staining and immunostaining images of CD45, CD68, CD8 and  $\alpha$ -SMA on tumour tissues. HCC, hepatocellular carcinoma; TME, tumour microenvironment.

patterns. Enrichment analysis revealed that HCCs highly expressed cell cycle associated genes than ICC, while type IV not other three types HCC displayed analogous downregulated pathways to ICC (figure 3M and online supplemental figure 11). Additionally, according to Bagaev's classification for cancers, only type IV HCC can be identified as having an 'immune-enriched and fibrotic' tumour microenvironment (TME), while types II and III are characterised by a depleted TME, and type I tumours have either immune-enriched or depleted TME features (figure 3N).<sup>17</sup> Histological examination revealed an increase in infiltrated leukocytes (CD45<sup>+</sup> cells) in HCCs with type IV. However, within these infiltrating cells, there appeared to be a predominance of macrophages (CD68<sup>+</sup> cells) rather than CD8<sup>+</sup> T cells (figure 4). We further confirmed the presence of differences in TME-related factors, including VEGFA, VEGFC, CD34, PDGFRA, PDGFRB, TGF $\beta$ 1 and HGF across different gross subtypes. Higher expression levels of VEGFA and TGF $\beta$ 1 were identified in the type IV group compared with other groups. Additionally, the CD34-positive blood vessels in type IV HCCs appeared dilated and longer compared with HCCs with other subtypes (online supplemental figure 12).

### Non-tumour tissues of patients with type IV HCC are characterised by immunosuppressive microenvironment

When comparing the microenvironment score between tumour tissues and non-tumour tissues, the differences in type IV HCC are comparatively less pronounced than those observed in other subtypes (online supplemental figure 13A). The dendrogram analysis revealed that 75% of non-tumour tissues were clustered into a single group, while 75% (6/8) of the non-tumour tissues in the type IV group could be grouped into one cluster (online supplemental figure 13B). Notably, we identified 308 downregulated DEGs in type IV non-tumour samples compared with the samples of the other three types, the majority of which were enriched in immune-related pathways, such as antigen processing and presentation, and lymphocyte activation (online supplemental figure 13C,D). Furthermore, our GSEA results, using hallmark gene sets, demonstrated a decrease in inflammatory response, complement, IL2-Stat5 signalling and EMT, along with upregulation of fatty acid metabolism and oxidative phosphorylation (online supplemental figure 13E-J).

### Genomic landscape of HCC with different gross classification

Analysis of gene mutations in the cohort of 49 patients revealed TTN (45%), TP53 (43%), MUC16 (22%), CTNBN1 (20%) and TRPA1 (20%) as the top five frequently mutated genes. The observed mutation frequencies of TP53 were significantly higher in type IV HCC samples (66.7%) than those in type I, type II and type III HCC samples (30.8%, 25.0% and 50.0%, respectively) (figure 5A). Notably, TP53 was identified as the main significantly mutated gene across all subtypes except for type I HCC (figure 5B). No significant differences in tumour mutation burden harboured by HCC were detected among different groups (figure 5C). Mutational signatures of each sample are shown in figure 5D,E, and no significant differences in signatures were observed among different subtypes. Three mutational signatures across all samples, namely, COSMIC signature 5, signature 16 and signature 22, were calculated and identified (figure 5F). Previous studies have suggested that tumours exhibiting an aristolochic acid signature (signature 22) have a higher number of infiltrating CD8<sup>+</sup> T cells,<sup>18</sup> the abundances of immune cells with/without specific signature fails to reach statistical significance (figure 5G). Structure variations were shown in figure 5H.

### Altered HCC gross classification associated gene expression contributed by copy number variation

The probabilistic scoring of amplification and deletion alterations in chromosome regions is depicted in figure 6A,B. Notably, no significant enrichment of alterations was detected in any of the gross subtypes. To identify altered genes in each chromosome region, copy number variation (CNV)-mRNA correlation analysis was employed, as shown in figure 6C. Following an overlap with upregulated DEGs of tumours with different gross subtypes, type IV HCCs were found to be enriched with 12 gene amplifications, as illustrated in figure 6D. It is noteworthy that UCK2 and DSN1 were amplified across all HCC subtypes. Additionally, four, three, nine and two genes were identified as deletion genes in types I-IV HCCs, respectively (figure 6E). Furthermore, the correlated expressions of CR1 and FOSB were detected across all gross classifications.

### Functional modules and hub genes of HCC associated with different gross subtypes

Using weighted correlation network analysis (WGCNA), a total of 12 gene modules were determined, as illustrated in figure 7A.

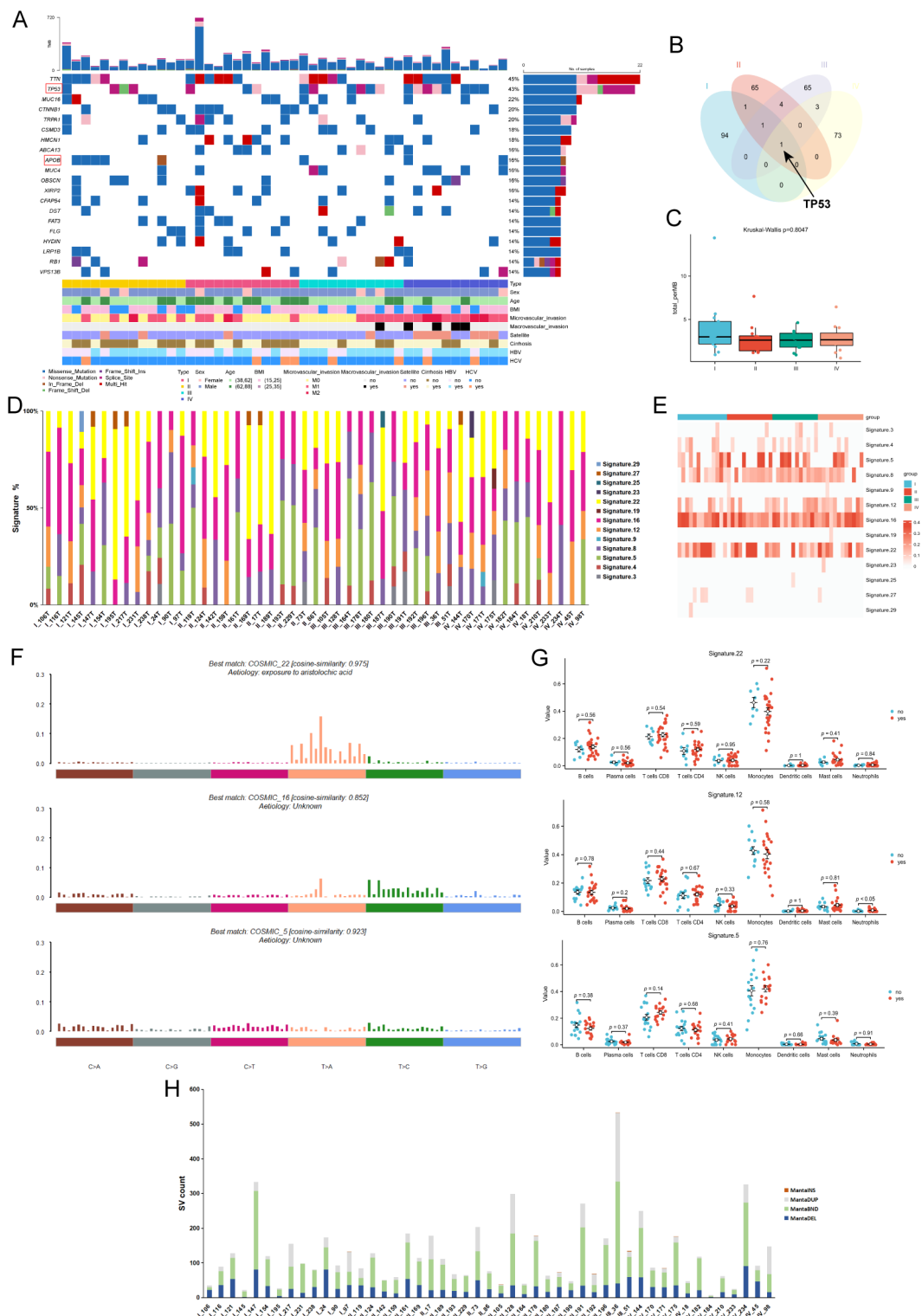


**Figure 5** Whole-genomic landscape of the current HCC cohort. (A) Somatic gene profile and indicated clinical variables of 49 HCC tumours. Red frames representing the difference frequencies of alterations in TP53 and APOB among the four gross subtypes. (B) Venn diagram showing significant gene mutations and overlaps among the four gross subtypes ( $p < 0.05$ ). (C) Box plot depicting the comparisons of TMB across the gross subtypes. (D) The relative weight of mutational signatures in individual samples. (E) Heatmap for the estimated confidence value of mutational signatures in each sample. (F) The mutational signature activities of corresponding extracted mutational signatures (signature 22, 16 and 5) in all samples. The 96-trinucleotide mutation patterns involved in six base substitution types were on the x-axes, while the percentage of mutations in the signature ascribed to individual mutation type were on the y-axes. (G) Dot plot displaying the abundances of immune cells in tumours with or without indicated signatures (Wilcoxon rank sum test). (H) Stacking diagram showing the number and types of SVs. HCC, hepatocellular carcinoma; SVs, structure variations.

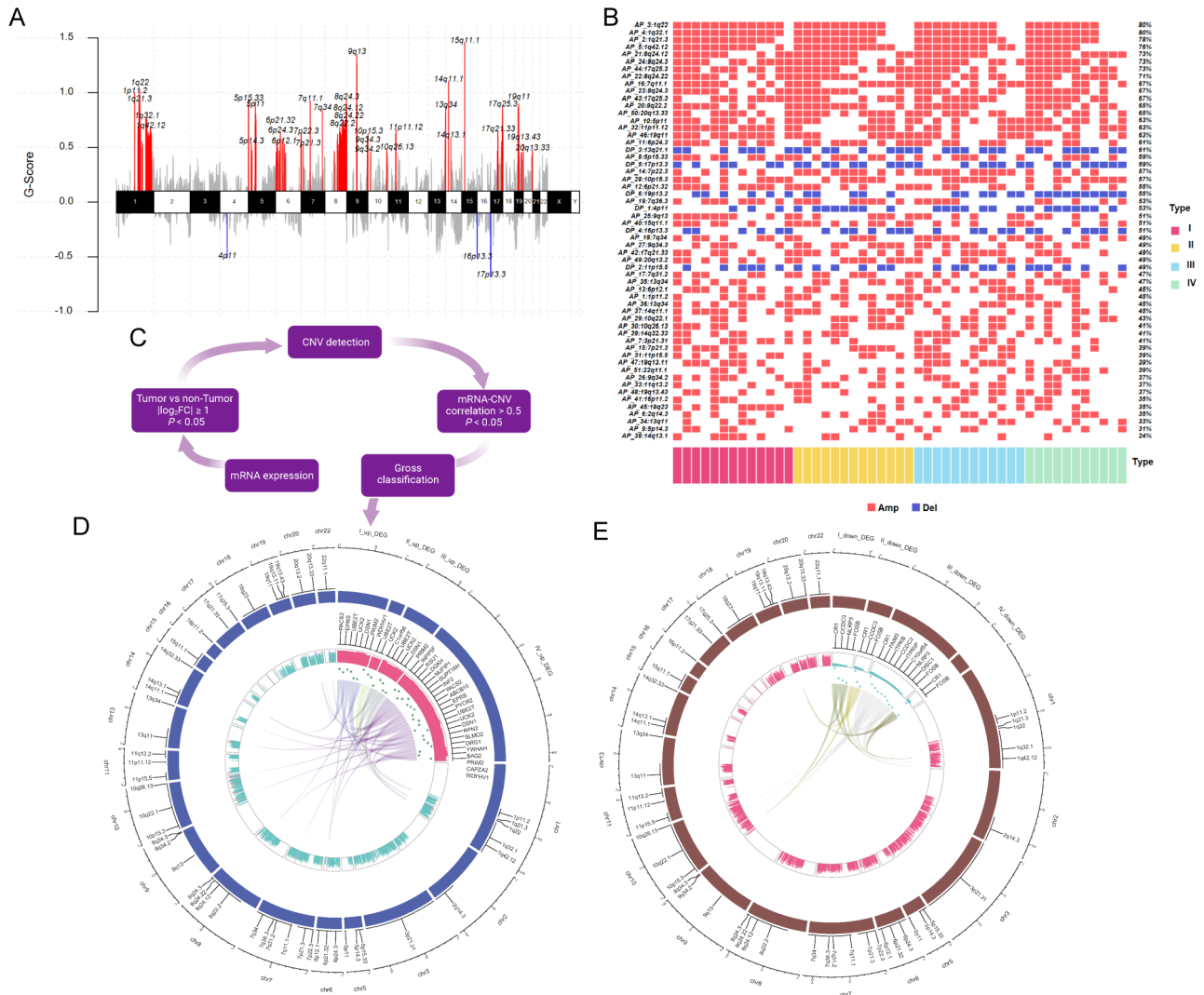


**Figure 6** Altered HCC gross classification associated gene expression contributed by CNV. (A) CNV across all samples in the current HCC cohort. GISTIC CNV analysis displaying the amplification (red) and deletion (blue) of multiple chromosomal regions. (B) Heatmap for CNV of all chromosomal regions among the four gross subtypes. The percentages of corresponding CNV were indicated. (C) Workflow for identifying gross type associated CNV-mRNA correlated genes. (D–E) Circos plot showing CNVs and their correlated mRNAs. The outer circle indicated CNVs locations across all autosomes. The frequencies of somatic copy number gains (D) and losses (E) as well as the correlations (Pearson correlation) between CNV and mRNA expression were shown in the inner circles. The gene symbols were shown. AP, amplification; CNV, copy number variation; DP, deletion; HCC, hepatocellular carcinoma.

The MEpink module exhibited a positive correlation with gross subtype (correlation 0.43,  $p=0.007$ ), microvascular invasion (correlation 0.55,  $p=0.0003$ ), macrovascular invasion (correlation 0.33,  $p=0.04$ ), satellite (correlation 0.42,  $p=0.007$ ), recurrence (correlation 0.39,  $p=0.02$ ) and death (correlation 0.36,  $p=0.02$ ). Conversely, the MEred module was negatively associated with microvascular invasion (correlation  $-0.49$ ,  $p=0.001$ ), AFP value (correlation  $-0.47$ ,  $p=0.003$ ), and death (correlation  $-0.33$ ,  $p=0.04$ ) (figure 7B). The findings presented in figure 7C demonstrated that the gene modules significantly related to type IV HCC were MEpink (correlation 0.67,  $p=3e-06$ ), MEbrown (correlation 0.56,  $p=2e-04$ ) and METurquoise (correlation 0.45,  $p=0.004$ ). Moreover, hierarchical clustering analysis revealed that these three modules exhibited more prominent coexpression patterns among themselves compared with other modules (online supplemental figure 14A). As such, we identified the genes in these three modules together with CNV-mRNA correlated genes as the ‘malignant gene set (MGS)’. GO and KEGG analysis

showed that the MEpink module containing 194 genes were enriched in GO pathways including macrophage activation and cell development, and KEGG pathways such as tyrosine metabolism (figure 7D,E and online supplemental figure 14). MEbrown module genes were enriched in TME remodelling associated pathways such as extracellular matrix organisation, regulation of angiogenesis and response to TGF- $\beta$  (figure 7D,F). The enrichment analysis of METurquoise module revealed that these genes were primarily associated with immune-related pathways (figure 7D,G). MEred module was characterised as metabolic process related module (figure 7D,H). The genes were included in MEGreenyellow module and enriched into response to metal ion (online supplemental figure 14B). The module eigengene (ME) values of pink, brown and turquoise were higher in type IV HCC than the other groups, while the ME value of red was lower. Turquoise and brown modules had decreased ME values in type II and type III HCCs (figure 7E,G). The hub genes of specific in each gross type identified by the module membership

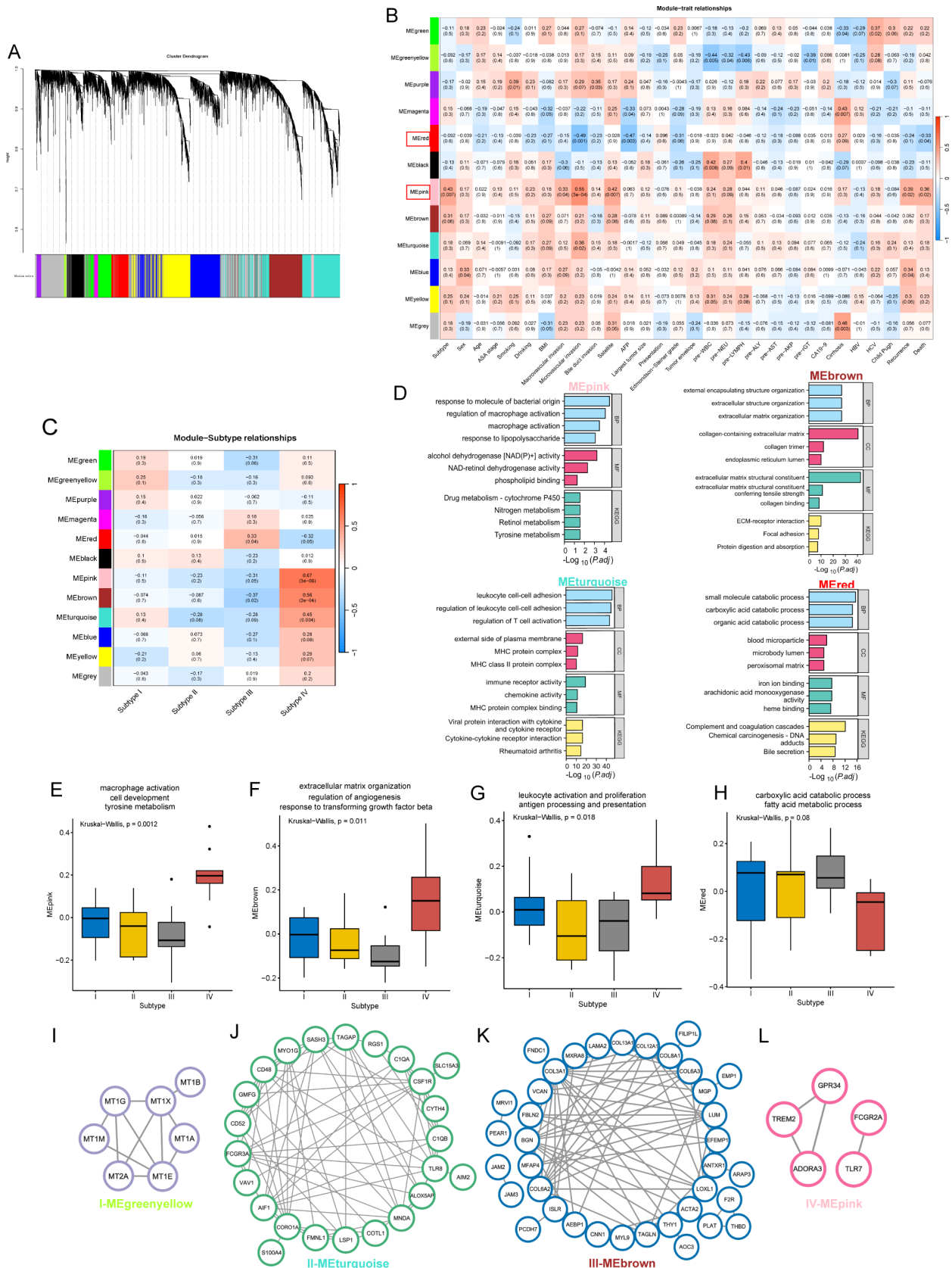


**Figure 7** Specific gross subtype-related modules identified by WGCNA. (A) Cluster dendrogram of mRNA and coexpression network module colours. (B) Correlations of the modules with clinical variables. (C) Correlations of the modules with the four gross subtypes. (D) Bar plot depicting the top enriched GO and KEGG pathways of gross subtype correlated modules ( $p < 0.05$ ). (E–H) Box plot showing the comparisons of the indicated module eigengene values across the four gross subtypes (Kruskal-Wallis test). The main functions of each module were annotated. (I–L) The protein–protein interactions using hub genes screened by the module membership (absolute values  $> 0.8$ ) and gene significance (absolute values  $> 0.2$  or  $0.3$ ) with regard to each gross subtype, respectively, and visualised by cytoscape. ME, module eigengene; WGCNA, weighted correlation network analysis.

(MM) value and gene significance (GS) value were shown in (figure 7I–L, online supplemental figure 14 and online supplemental table 3).

### Prognostic prediction model for HCC based on MGS

To enhance the practicality and generalisability of this gross classification, we integrated MGS and developed a prognostic prediction model for HCC based on data from TCGA-LIHC cohort. LASSO regression analysis was employed, resulting in a development of a HCC prognosis risk score model consisting of 18 genes (termed as ‘HEPAR-18’). Importantly, our model demonstrated excellent performance, with area under the curve (AUC) values of 0.810, 0.764 and 0.780 for predicting survival probability at 1-year, 2-year and 3-year intervals, respectively (figure 8A–C). Each variable in this model can significantly distinguish the survival benefits of individuals (figure 8D and online supplemental figure 15). A subsequent multivariate Cox regression analysis revealed that all 18 genes in the ‘HEPAR-18’ model were independent risk factors for HCC and the coefficient values were shown in figure 8E. The Risk Score were evaluated following the gene expression, subsequently the distribution of Risk Score and corresponding survival event of each individual in the training cohort were described. As demonstrated in figure 8F,G, the patients with high Risk Score were demonstrated with inferior survival benefits. Meanwhile, the AUC values of HEPAR-18 and TNM stage were 0.776 vs 0.674 (figure 8H). The samples at TNM III/IV were presented with higher Risk Score (figure 8I). Same tendencies are robustly confirmed in the validation sets: International Cancer Genome Consortium cohort (figure 8J–M), HBV-related HCC cohort (figure 8N–Q) and the current cohort (figure 8R,S). Furthermore, the samples with larger tumour size and at BCLC intermediate/advanced stage were presented with higher Risk Score using the HBV-related HCC cohort (figure 8T,U).

### Gross classification would be a valuable tool guiding HCC therapy

The histology of type IV HCC was distinguished by high stroma content (eg, CAFs, vessels) and increased immune cell infiltration, especially monocytes and macrophages (figure 4, figure 9A), while relatively infiltrated-depleted TME was observed in the HCC with type II or type III, which was consistent with the transcriptomic findings discovered by GSVA and xCell (figure 2E–K). To further explore the clinical value of HCC gross subtypes and their molecular characteristics, we initially compared the efficacy of adjuvant TACE treatment in patients undergoing partial hepatectomy for different gross subtypes of HCC. As successful TACE efficacy requires that the tumour has sufficient nutrient vessels, we found that postoperative TACE improved OS in type IV HCC as expected (475.3 days vs 640.1 days,  $p=0.065$ ). Given that the potential presence of more severe disease in the TACE group, our analysis confirmed significantly beneficial effects of adjuvant TACE therapy on OS after correcting confounding factors using stabilised IPTW ( $p=0.039$ ) (figure 9B). The therapeutic effects on HCC were not significant in the Type I/II/III group before or after adjustment by IPTW (figure 9C).

We also encompassed another prospective cohort containing 79 patients with advanced HCC, who received immunotherapy combined with antiangiogenesis targeted therapy as their primary treatment modality. The gross subtype of each tumour was evaluated by two radiologists using enhanced CT/MRI, with blinding to the outcomes of patients. The majority of patients (81%) in this cohort harboured at least one type IV nodule with a

higher incidence of macrovascular invasion (59.4% vs 46.7% for other three types). The objective response rate (ORR) in patients with type IV HCC (30%) were seemingly slightly higher compared with the patients with type II/III (20%), although shortened survival benefits were still observed in patients with type IV HCC (figure 9D). In a small subset of patients (12 patients) with type IV and non-type IV HCC nodules simultaneously, better response to immune checkpoint blockade therapy combined with antiangiogenesis targeted therapy in type IV than other type was found in some cases (figure 9E). Type III HCCs can be further classified into two subtypes: type IIIA, characterised by confluent multiple nodules without any extranodular parts, typically exhibiting a regular round smooth margin; and type IIIB, characterised by confluent multiple nodules with extranodular parts, usually with irregular margin (online supplemental figure 16A). These two subtypes of type III HCCs have distinct patterns of gene expression and differences in survival outcomes (online supplemental figure 16B–D).

### DISCUSSION

Clinical staging for HCC based on imaging findings is extensively used, such BCLC staging system, which often requires clinicians to make treatment decisions without a histological diagnosis.<sup>17–19</sup> However, current guidelines based on these staging systems often lack specific management recommendations for patients with solitary HCC, especially those less than 5 cm in size (BCLC stage 0/A).<sup>2,20</sup> To date, no consistent conclusions have been reached regarding the preference of treatment strategies such as surgical or ablative treatment in these patients.<sup>21–23</sup>

Gross classification, endorsed by LCGSJ and Korean Liver Cancer Association, shows promise to stratify HCC management, but it has yet to gain widespread adoption in clinical settings.<sup>8,24</sup> In this study, we constructed a relatively large prospective cohort of 400 surgical patients with solitary HCC with different gross subtypes. Types II and III HCC were demonstrated to have worse OS and RFS than type I, while type IV HCC presented the worst prognosis. Although similar trends were observed in previous studies, the differences were not found to be statistically significant due to lack of samples with specific subtype of HCC or multiple nodules.<sup>10,11,25</sup> Particularly, type IV HCC is very rare in Japanese patient cohorts, who more commonly suffer from HCV.<sup>14</sup> In contrast, it appeared to be relatively frequent among Korean and Chinese HCC patient cohorts, which are predominantly associated with HBV infection.<sup>10,11</sup> As such, the distribution of HCC gross classification may be influenced by different aetiologies.

Consistent with previous studies, our study confirmed that histopathological features including vascular invasion, micrometastasis or tumour size increased in severity in the order of type I, type II/III to type IV.<sup>10,26</sup> Therefore, in non-type I HCC (especially type IV), hepatic resection which can achieve more extensive excision than other curative-intent modalities, would be preferred.<sup>14</sup> The differences in patient’s outcomes between type II/III and type I HCCs were no longer significant, those between type IV and the other three gross subtypes remained significant after IPTW adjustment. These findings suggest that type IV HCC may involve undiscovered mechanisms contributing to its aggressive features.

In current study, HCC tumours demonstrated downregulated metabolic pathways, with the most significant alterations observed in type IV. This subtype displayed a similar transcriptional profile to the most malignant molecular subtype S-Pf defined in a previous study.<sup>27</sup> We further revealed that lipid

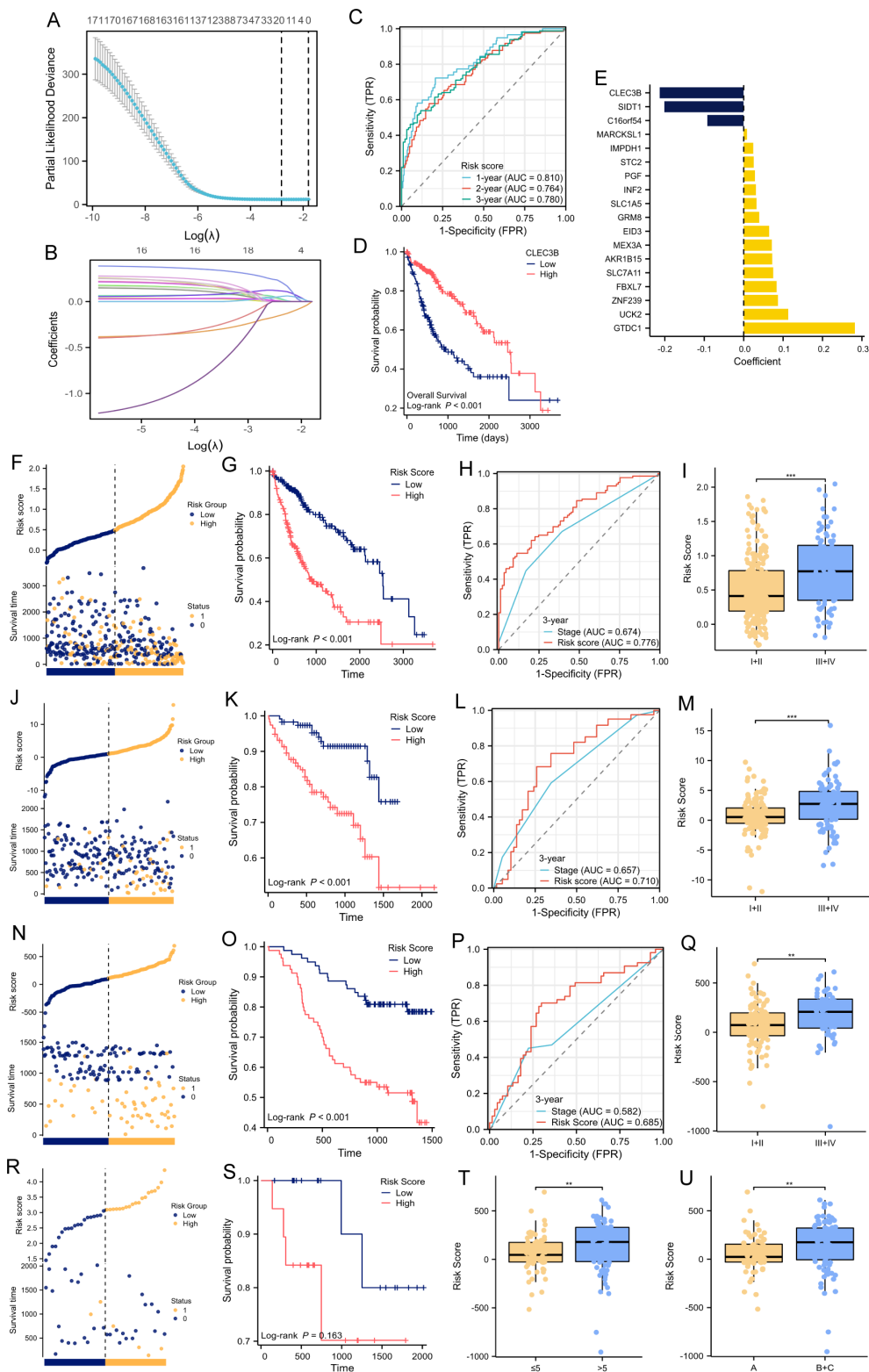


**Figure 8** Prognostic prediction model for HCC based on MGS. (A) Lambda selection in the LASSO model using TCGA-LIHC cohort as the training cohort. (B) LASSO coefficient profiles of the 18 included genes. (C) The 1-year, 2-year, 3-year AUC of predicting death using HEPAR-18 among patients in TCGA-LIHC cohort. (D) The Kaplan-Meier survival curve of CLEC3B in TCGA-LIHC cohort (log-rank test). (E) The coefficients of the 18 included genes. (F–I) In TCGA-LIHC cohort. (J–M) In ICGC validation cohort. (N–Q, T, U) In HBV-related HCC validation cohort. (R–S) In current HCC cohort. (F, J, N, R) Distribution of Risk Score and survival status of HEPAR-18. (G, K, O, S) The Kaplan-Meier survival curve of HEPAR-18 (log-rank test). (H, L, P) Comparisons of the 3-year AUCs of TNM staging and HEPAR-18 in predicting death among patients. (I, M, Q) Box plot showing the comparison of Risk Score using HEPAR-18 between patients with early stage (I/II) and advanced stage (III/IV). (T) Box plot displaying the comparison of Risk Score using HEPAR-18 between patients with tumour size  $>5$  cm and  $\leq 5$  cm. (U) Box plot displaying the HEPAR-18 Risk Score patients at BCLC stage A versus BCLC stage B and C (Wilcoxon rank sum test, \*\*  $p < 0.01$ , \*\*\*  $p < 0.001$ ). AUC, area under the curve; HCC, hepatocellular carcinoma; ICGC, International Cancer Genome Consortium.

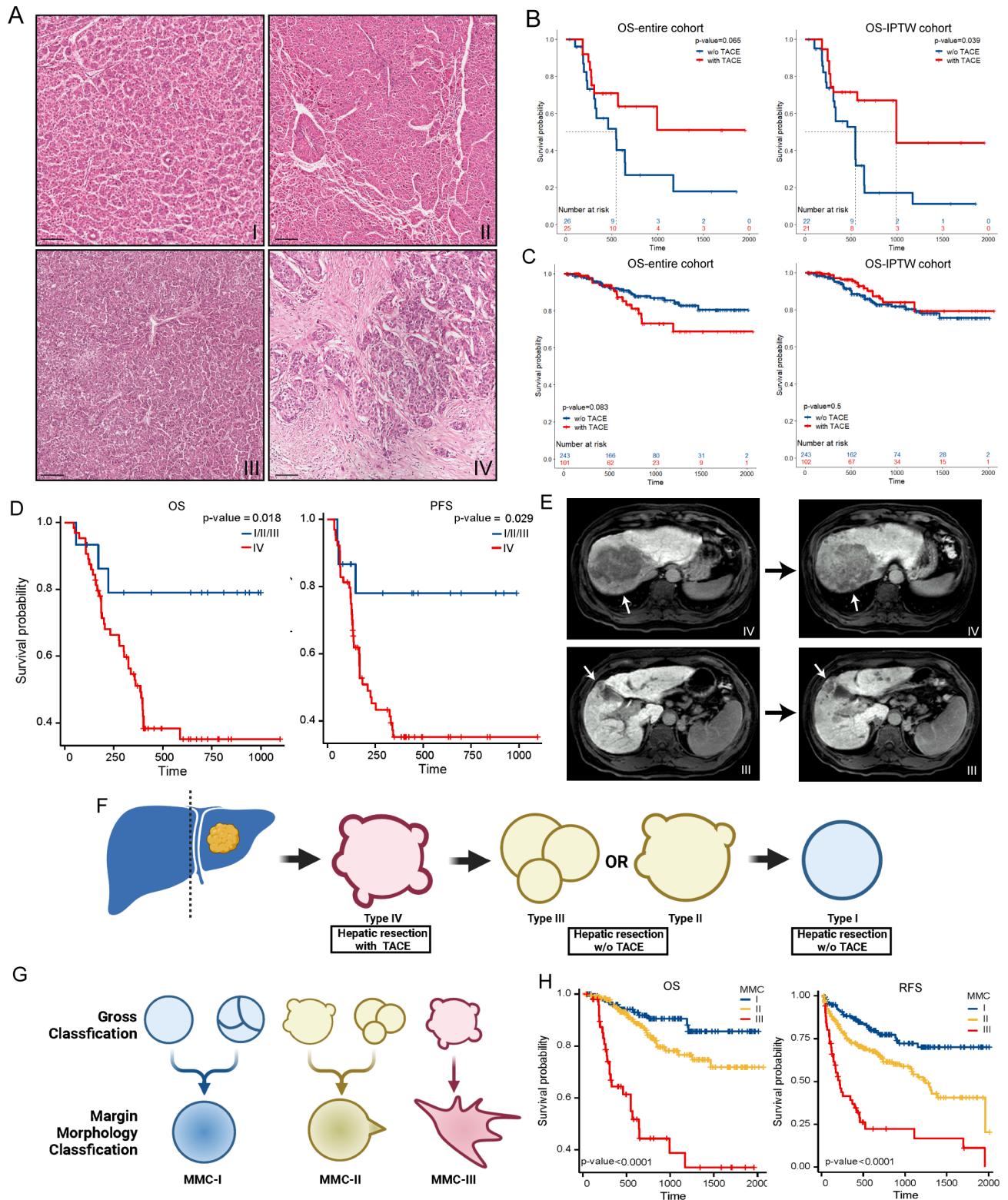


**Figure 9** Gross classification guiding HCC therapy. (A) H&E staining of HCC tumour samples of all gross types. (B) The Kaplan-Meier curves of OS in patient with type IV HCC treated with or without TACE postoperatively in current overall cohort or IPTW cohort (log-rank test). (C) The Kaplan-Meier curves of OS in patient with type I/II/III HCC treated with or without TACE postoperatively in the overall cohort or IPTW cohort (log-rank test). (D) The Kaplan-Meier curves of OS and PFS in patient with type I/II/III HCC treated with or without adjuvant drug therapies postoperatively in the overall cohort or IPTW cohort (log-rank test). (E) Gd-EOB-DTPA MRI for the patient with HCCs with type III and type IV before and after immunotherapy combined with antiangiogenesis targeted therapy. White arrows indicated HCC nodules. (F) The clinical implementation process for gross classification of resectable HCC and the corresponding recommended treatment strategies. (G) A novel trichotomous classification system, margin morphology classification (MMC) was proposed based on the conventional gross classification. (H) OS or RFS of patients undergoing hepatic resection for HCCs with different MMC subtype (log-rank test). HCC, hepatocellular carcinoma; IPTW, inverse probability of treatment weight; OS, overall survival; RFS, recurrence-free survival; TACE, transcatheter arterial chemoembolisation.

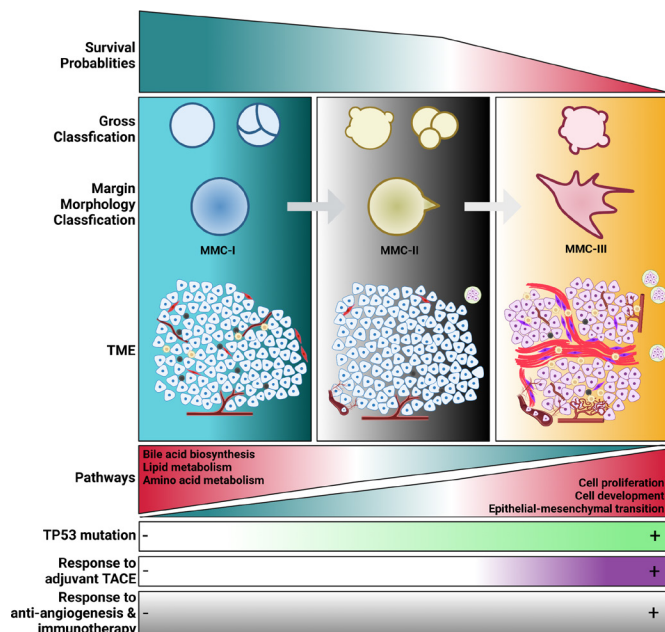


**Figure 10** Graphical overview of HCCs with gross classification subtypes and corresponding MMC subtypes. MMC-I includes type I and IIIA, while MMC-II includes types II and IIIB. MMC-III indicates type IV. Patients with MMC-I HCCs have a better survival rate than those with MMC-II, while MMC-III showed the worst prognosis. Different TME and expressional patterns were shown. HCCs with MMC-III exhibit higher levels of vascular invasion and microsatellite proportions, as well as a higher incidence of TP53 mutation. MMC-III HCCs also show a better response to adjuvant TACE compared with HCCs with other subtypes. Although higher objective response rate to the combination of antiangiogenesis targeted therapy and immunotherapy was found in advanced MMC-III HCCs, their prognosis remained worse compared with those only with other subtypes of nodules. Further studies are required to draw clear conclusions. HCC, hepatocellular carcinoma; MMC, margin morphology classification; TACE, transcatheter arterial chemoembolisation; TME, tumour microenvironment.

metabolism enriched red module was significantly negatively associated with type IV, recurrence and death by WGCNA analysis. To date, only a few genes involved in different metabolism pathways (eg, ALDOB, GSTZ1 and CPT2) have been identified as tumour suppressors in HCC.<sup>28–30</sup> Our findings support that reprogramming the intrinsic metabolic capacity of cancer has the potential to provide therapeutic opportunities.<sup>31</sup> Deciphering the metabolic features of distinct cellular components within TME would be critical to achieve specific elimination of cancer cells while preserving immune cell activity simultaneously.<sup>32,33</sup>

Furthermore, we delineated the organisation of TME for each gross subtype HCC spatially and transcriptomically: Type IV HCC is characterised by fibrotic or immune-enriched fibrotic TME, while type II/III has features of depleted TME. Type I HCC is distinguished by depleted or immune-enriched TME. Conversely, the previous study suggests HCC with depleted TME subtype calculated only based on RNA-seq data exhibited inferior prognosis than other TME subtypes,<sup>34</sup> which may result from the limitations of predicting components based only on gene expression.

Of note, type IV HCC exhibits similar macroscopic features (greyish white, tough and poorly defined) and postoperative prognosis to those of ICC (median OS: 634 days) in our centre. Type IV HCC presented with the highest frequency of TP53

mutations (66.7%), and with the greatest similarity to ICC in terms of downregulated gene enrichment pathways across the four gross subtypes, possessing molecular features reminiscent of the recently identified ICC-like subtype,<sup>35</sup> which is partially identified with significant downregulated bile acid metabolic pathways and TP53 mutation. TP53 mutations can induce the dedifferentiation of mature hepatocytes into progenitor-like cells and potentially contribute to the formation of ICC-like HCC.<sup>36</sup> While bile acid is reported to contribute to HCC oncogenesis in the context of Mst1/2 or Sirt5 knockout genomic background,<sup>37,38</sup> the role of bile acid metabolism in driving HCC progression warrants further exploration. On the other hand, we found the somatic mutations in type IV HCC are distinct from those observed in ICC. For instance, FGFR2 fusion mutation which was prevalent in ICC is not detected in type IV HCC.<sup>39</sup> In future research, it is crucial to prioritise the exploration of the relationship and distinctions between the tumour components in combined HCC-ICC and type IV HCC.

Our analysis first revealed a type IV strongly correlated ‘pink module’, which also exhibited the strongest positive correlation with aggressive behaviours of HCC by WGCNA, suggesting its crucial role in driving HCC progression. Four alcohol dehydrogenase genes ADH1A, ADH1B, ADH1C and ADH6 are included in it, while ADH1A was already shown to be a prognostic marker for HCC and negatively correlated with cell proliferation.<sup>27,40</sup> Together with the higher abundance of macrophages detected histologically in type IV HCC, three hub genes of pink module, TLR7, GPR34 and TREM2 are primarily enriched in macrophages (<http://www.proteinatlas.org/>),<sup>41</sup> suggesting the pivotal involvement of macrophages in promoting invasive and metastasis. TLR7 is regarded as a molecular marker for M2-type tumour associated macrophages. The potential therapeutic value of activating TLR7 in HCC and ICC has been investigated in clinical trials (NCT04338685).<sup>42</sup> The increase of Trem2<sup>+</sup> macrophages after TACE treatment suppresses recruitment of CD8<sup>+</sup> T cells to the tumour lesion, potentially contributing to HCC recurrence.<sup>43</sup> Further investigation into targeting diverse populations of macrophages in advanced HCC is necessary.<sup>44</sup> Collectively, we believe that gross classification may aid in assessing the TME, especially in immunophenotyping TME throughout HCC cancer stages. Moreover, devising strategies specifically targeting cell groups tailored to distinct gross subtypes would be promising after obtaining a deeper understanding of immune clusters in the future.

Previous studies have shown that adjuvant TACE did not improve the prognosis of patients undergoing hepatectomy for large HCC.<sup>45</sup> Intriguingly, our study found that adjuvant TACE prolonged the prognosis of patients in type IV subgroup, but not for patients with the other three types when compared with hepatectomy alone. Actually, more occult micrometastases outside the surgical region can be detected by digital subtraction angiography in patients with type IV HCC. In addition, we found the satellite nodules in type IV exhibit a highly vascularised TME histologically, which may enhance their responsiveness to TACE. Collectively, adjuvant TACE should be considered for patients with type IV HCC. However, TACE alone would not be recommended for treating non-type I HCC.<sup>13</sup>

A previous study showed that in unresectable patients, type 4 HCC (similar to type IV here) were more likely to achieve an overall response to antiangiogenesis drug lenvatinib.<sup>46</sup> The majority of patients in our non-resectable HCC cohort were found to have type IV nodules. Despite attaining higher ORR to the combination of antiangiogenesis targeted therapy and immunotherapy in type IV HCCs, their prognosis remained worse

compared with those only with other three subtypes of nodules. Including more patients would help to clarify the issue. Immunotherapy together with locoregional treatment (eg, TACE) might be propitious in type IV HCC, which has been shown to be effective for advance HCC in a single-arm phase II study.<sup>47</sup>

To promote the clinical application of gross classification, we recommend evaluating HCC gross classification based on fresh tissue specimens with a priority assessment for type IV in treatment decision-making (figure 9F). Considering the similarities in pathology, molecular features, and prognosis between type II and type III HCC, we propose a modified gross classification system MMC for HCC based solely on margin morphology. The MMC system includes: MMC-I (smooth type), nodules with smooth near-rounded margins including gross classification type I and type IIIA; MMC-II (extranodular growth type), nodules with extranodular margins comprising  $\leq 50\%$  of the tumour circumference, or  $\leq 3$  directions, including type II and type IIIB; and MMC-III (infiltrative type), infiltrative nodules with irregular margins comprising  $>50\%$  of the tumour circumference, or  $>3$  directions, including type IV (figure 9G–H). In clinical practice, priority should be given to assessing whether the HCC nodule belongs to MMC-III.

In conclusion, our study reveals significant differences in molecular and pathological characteristics as well as prognosis among different gross subtypes of HCC (figure 10). These findings provide a biological basis and clinical rationale for the development of personalised and precise treatment plans for HCC. Furthermore, we propose that gross classification, which can be easily obtained by radiological examinations, can serve as a foundation for refined stratified management of HCC.

**Acknowledgements** We would like to express our sincere gratitude to Professor Run-Sheng Chen's team for their valuable assistance and support during the research. We wish to acknowledge the technical assistance provided by Professor Shu-Li Xie and Dr. Ming-Qian Li. We want to appreciate Dr. Meng-Han Gao for language polishing and logical organisation. We would like to thank Jia-Ao Yu, Shu-Xuan Li, Shi-Fei Song, Kai Kou and Xing Lv for their hard work in collecting samples. We thank the Department of Biobank, Division of Clinical Research, First Hospital of Jilin University for constructing tissue microarray. We also would like to appreciate Professor Yan-Hua Wu and Professor Jing Jiang for statistical supports. Some published data used in this study was generated by the TCGA Research Network: <https://www.cancer.gov/tcga>. A few figures were generated on BioRender.com.

**Contributors** Conception: GL, ZF and GW; study design: ZF, MJ, LZ and NW; administrative support: GL, GW, LQ and HZ; data collection and acquisition: ZF, MJ, LZ, CW, HW, PZ, FW, XD, XSun, WQ, MW, XShi, JY, CJ, JZ, WC, BH, KC, YC, WM, YH, YL, GW, TL and JQ; data analysis: ZF, MJ, ML and YH; manuscript preparation: ZF, MJ and ML; critical revision: TY and GL; guarantor: GL; final approval of manuscript: all authors.

**Funding** This study was supported by the Natural Science Foundation of Jilin Province (No. YDZJ202201ZYTS014) and Natural Science Foundation of China (No. 81602059, 82241223 and U20A20360), Foundation of Health Commission of Jilin Province (No. 2018J052).

**Competing interests** None declared.

**Patient and public involvement** Patients and/or the public were not involved in the design, or conduct, or reporting, or dissemination plans of this research.

**Patient consent for publication** Not applicable.

**Ethics approval** This study was conducted in accordance with the Declaration of Helsinki and the Ethical Guidelines for Clinical Studies, and approved by the Institutional Review Boards of First Hospital of Jilin University (No: 2020-675-1).

**Provenance and peer review** Not commissioned; externally peer reviewed.

**Data availability statement** The datasets analysed during the current study are available from the corresponding author on reasonable request.

**Supplemental material** This content has been supplied by the author(s). It has not been vetted by BMJ Publishing Group Limited (BMJ) and may not have been peer-reviewed. Any opinions or recommendations discussed are solely those of the author(s) and are not endorsed by BMJ. BMJ disclaims all liability and responsibility arising from any reliance placed on the content. Where the content

includes any translated material, BMJ does not warrant the accuracy and reliability of the translations (including but not limited to local regulations, clinical guidelines, terminology, drug names and drug dosages), and is not responsible for any error and/or omissions arising from translation and adaptation or otherwise.

**Open access** This is an open access article distributed in accordance with the Creative Commons Attribution Non Commercial (CC BY-NC 4.0) license, which permits others to distribute, remix, adapt, build upon this work non-commercially, and license their derivative works on different terms, provided the original work is properly cited, appropriate credit is given, any changes made indicated, and the use is non-commercial. See: <http://creativecommons.org/licenses/by-nc/4.0/>.

#### ORCID iDs

Tian Yang <http://orcid.org/0000-0002-8333-3673>

Guoyue Lv <http://orcid.org/0000-0003-4656-4955>

#### REFERENCES

- Vogel A, Cervantes A, Chau I, et al. Hepatocellular carcinoma: ESMO clinical practice guidelines for diagnosis, treatment and follow-up. *Ann Oncol* 2018;29:iv238–55.
- Vogel A, Martinelli E, et al. ESMO Guidelines Committee. Electronic address: [clinicalguidelines@esmo.org](mailto:clinicalguidelines@esmo.org). Updated treatment recommendations for hepatocellular carcinoma (HCC) from the ESMO clinical practice guidelines. *Ann Oncol* 2021;32:801–5.
- Benson AB, D'Angelica MI, Abbott DE, et al. Hepatobiliary cancers, version 2.2021. NCCN clinical practice guidelines in oncology. *J Natl Compr Canc Netw* 2021;19:541–65.
- Salem R, Tselikas L, De Baere T. Interventional treatment of hepatocellular carcinoma. *J Hepatol* 2022;77:1205–6.
- Finn RS, Qin S, Ikeda M, et al. Atezolizumab plus bevacizumab in unresectable hepatocellular carcinoma. *N Engl J Med* 2020;382:1894–905.
- Llovet JM, Pinyol R, Kelley RK, et al. Molecular pathogenesis and systemic therapies for hepatocellular carcinoma. *Nat Cancer* 2022;3:386–401.
- Sangro B, Melero I, Wadhawan S, et al. Association of inflammatory biomarkers with clinical outcomes in nivolumab-treated patients with advanced hepatocellular carcinoma. *J Hepatol* 2020;73:1460–9.
- Kanai T, Hirohashi S, Upton MP, et al. Pathology of small hepatocellular carcinoma. A proposal for a new gross classification. *Cancer* 1987;60:810–9.
- Cha SW, Sohn JH, Kim SH, et al. Interaction between the tumor microenvironment and resection margin in different gross types of hepatocellular carcinoma. *J Gastroenterol Hepatol* 2020;35:648–53.
- Rhee H, Chung T, Yoo JE, et al. Gross type of hepatocellular carcinoma reflects the tumor hypoxia, fibrosis, and stemness-related marker expression. *Hepatol Int* 2020;14:239–48.
- He J, Shi J, Fu X, et al. The Clinicopathologic and Prognostic significance of gross classification on solitary hepatocellular carcinoma after hepatectomy. *Medicine* 2015;94:e1331.
- Fu X, Mao L, Tang M, et al. Gross classification of solitary small hepatocellular carcinoma on preoperative computed tomography: prognostic significance after radiofrequency ablation. *Hepatol Res* 2016;46:298–305.
- Adhoute X, Pénaranda G, Raoul J-L, et al. Hepatocellular carcinoma macroscopic gross appearance on imaging: predictor of outcome after transarterial chemoembolization in a real-life multicenter French cohort. *Eur J Gastroenterol Hepatol* 2019;31:1414–23.
- Kudo M, Kawamura Y, Hasegawa K, et al. Management of hepatocellular carcinoma in Japan: JSH consensus statements and recommendations 2021 update. *Liver Cancer* 2021;10:181–223.
- Lee Y, Park H, Lee H, et al. The Clinicopathological and prognostic significance of the gross classification of hepatocellular carcinoma. *J Pathol Transl Med* 2018;52:85–92.
- Japan LCSGo. The general rules for the clinical and pathological study of primary liver cancer. *The Japanese Journal of Surgery* 1989.
- Vogel A, Meyer T, Sapisochin G, et al. Hepatocellular carcinoma. *Lancet* 2022;400:1345–62.
- Freeman RB. Transplantation for hepatocellular carcinoma: the Milan criteria and beyond. *Liver Transpl* 2006;12:S8–13.
- Xie D, Shi J, Zhou J, et al. Clinical practice guidelines and real-life practice in hepatocellular carcinoma: a Chinese perspective. *Clin Mol Hepatol* 2023;29:206–16.
- Zhou J, Sun H, Wang Z, et al. Guidelines for the diagnosis and treatment of hepatocellular carcinoma. *Liver Cancer* 2020;9:682–720.
- Coticchio M, Inchingolo R, Delvecchio A, et al. Radiofrequency ablation vs surgical resection in elderly patients with hepatocellular carcinoma in Milan criteria. *World J Gastroenterol* 2021;27:2205–18.
- Xia Y, Li J, Liu G, et al. Long-term effects of repeat hepatectomy vs percutaneous radiofrequency ablation among patients with recurrent hepatocellular carcinoma: a randomized clinical trial. *JAMA Oncol* 2020;6:255–63.
- Takayama T, Hasegawa K, Izumi N, et al. Surgery versus radiofrequency ablation for small hepatocellular carcinoma: a randomized controlled trial (SURF trial). *Liver Cancer* 2022;11:209–18.

- 24 Martins-Filho SN, Alves VAF. The strengths and weaknesses of gross and histopathological evaluation in hepatocellular carcinoma: a brief review. *Surg Exp Pathol* 2019;2.
- 25 Hui AM, Takayama T, Sano K, et al. Predictive value of gross classification of hepatocellular carcinoma on recurrence and survival after hepatectomy. *J Hepatol* 2000;33:975–9.
- 26 Nakashima Y, Nakashima O, Tanaka M, et al. Portal vein invasion and intrahepatic micrometastasis in small hepatocellular carcinoma by gross type. *Hepatol Res* 2003;26:142–7.
- 27 Gao Q, Zhu H, Dong L, et al. Integrated proteogenomic characterization of HBV-related hepatocellular carcinoma. *Cell* 2019;179.
- 28 Liu G, Wang N, Zhang C, et al. Fructose-1,6-bisphosphate aldolase B depletion promotes hepatocellular carcinogenesis through activating insulin receptor signaling and lipogenesis. *Hepatology* 2021;74:3037–55.
- 29 Li J, Wang Q, Yang Y, et al. Gstz1 deficiency promotes hepatocellular carcinoma proliferation via activation of the KEAP1/NRF2 pathway. *J Exp Clin Cancer Res* 2019;38:438.
- 30 Fujiwara N, Nakagawa H, Enooku K, et al. CPT2 downregulation adapts HCC to lipid-rich environment and promotes carcinogenesis via acylcarnitine accumulation in obesity. *Gut* 2018;67:1493–504.
- 31 Sahai E, Astsaturov I, Cukierman E, et al. A framework for advancing our understanding of cancer-associated fibroblasts. *Nat Rev Cancer* 2020;20:174–86.
- 32 Arner EN, Rathmell JC. Metabolic programming and immune suppression in the tumor microenvironment. *Cancer Cell* 2023;41:421–33.
- 33 Ghesquière B, Wong BW, Kuchnio A, et al. Metabolism of stromal and immune cells in health and disease. *Nature* 2014;511:167–76.
- 34 Bagaev A, Kotlov N, Nomie K, et al. Conserved pan-cancer microenvironment subtypes predict response to immunotherapy. *Cancer Cell* 2021;39:845–65.
- 35 Jeon Y, Kwon SM, Rhee H, et al. Molecular and radiopathologic spectrum between HCC and Intrahepatic cholangiocarcinoma. *Hepatology* 2023;77:92–108.
- 36 Tschaharganeh DF, Xue W, Calvisi DF, et al. P53-dependent nestin regulation links tumor suppression to cellular plasticity in liver cancer. *Cell* 2014;158:579–92.
- 37 Ji S, Liu Q, Zhang S, et al. FGF15 activates hippo signaling to suppress bile acid metabolism and liver tumorigenesis. *Dev Cell* 2019;48:460–74.
- 38 Sun R, Zhang Z, Bao R, et al. Loss of SIRT5 promotes bile acid-induced immunosuppressive microenvironment and hepatocarcinogenesis. *J Hepatol* 2022;77:453–66.
- 39 Braconi C, Roessler S, Kruk B, et al. Molecular perturbations in cholangiocarcinoma: is it time for precision medicine. *Liver Int* 2019;39 Suppl 1:32–42.
- 40 Ahmed Laskar A, Younus H. Aldehyde toxicity and metabolism: the role of aldehyde dehydrogenases in detoxification, drug resistance and carcinogenesis. *Drug Metab Rev* 2019;51:42–64.
- 41 Schöneberg T, Meister J, Knierim AB, et al. The G protein-coupled receptor GPR34—the past 20 years of a grownup. *Pharmacol Ther* 2018;189:71–88.
- 42 Cheng K, Cai N, Zhu J, et al. Tumor-associated macrophages in liver cancer: from mechanisms to therapy. *Cancer Commun (Lond)* 2022;42:1112–40.
- 43 Tan J, Fan W, Liu T, et al. TREM2<sup>+</sup> Macrophages suppress CD8<sup>+</sup> T-cell infiltration after transarterial chemoembolisation in hepatocellular carcinoma. *J Hepatol* 2023;79:126–40.
- 44 Guillot A, Tacke F. Spatial dimension of macrophage heterogeneity in liver diseases. *eGastroenterology* 2023;1:e000003.
- 45 Zhou W-P, Lai ECH, Li A-J, et al. A prospective, randomized, controlled trial of preoperative Transarterial Chemoembolization for Resectable large hepatocellular carcinoma. *Annals of Surgery* 2009;249:195–202.
- 46 Kawamura Y, Kobayashi M, Shindoh J, et al. Pretreatment heterogeneous Enhancement pattern of hepatocellular carcinoma may be a useful new Predictor of early response to Lenvatinib and overall prognosis. *Liver Cancer* 2020;9:275–92.
- 47 Chiang CL, Chiu KWH, Chan KSK, et al. Sequential Transarterial Chemoembolisation and stereotactic body radiotherapy followed by Immunotherapy as conversion therapy for patients with locally advanced, Unresectable hepatocellular carcinoma (START-FIT): a single-arm, phase 2 trial. *The Lancet Gastroenterology & Hepatology* 2023;8:S2468-1253(22)00339-9:169–78..